Enhancement of wear properties of a polyether ether ketone polymer by incorporation of carbon and glass fibers

Hamilton, Stephanie ; Munoz de Escalona, Patricia

Published in:
Journal of Applied Polymer Science

DOI:
10.1002/app.47587

Publication date:
2019

Document Version
Author accepted manuscript

Enhancement of Wear Properties of a Polyether Ether Ketone (PEEK) Polymer by Incorporation of Carbon and Glass Fibres

Stephanie Hamilton[1], Patricia Muñoz-Escalona[2]*

*Corresponding Author

Patricia Muñoz-Escalona. Glasgow Caledonian University. G40BA.

Patricia.munoz@gcu.ac.uk

Abstract: Some properties of polymers can be improved through the incorporation of carbon and glass fibres into the polymer matrix. In this research the wear resistance of two polymer composites CF-PEEK and GF-PEEK were compared with the virgin PEEK. The wear resistance was assessed by Pin on Disk tests performed using a range of reinforced polymer pins tested against a steel disk. The influence of load, sliding velocity, counter-surface hardness and reinforcement concentration and type, on the specific wear rate was investigated. The materials were chosen to simulate the wear experienced between a polymeric anti-extrusion ring and a steel sealing surface utilized within valves in the oil and gas industry. The average mass loss was recorded and an Analysis of the Variance carried out to investigate the contribution of each parameter on specific wear rate. Results showed that wt.% reinforcement and type of reinforcement material were primary contributors towards specific wear rate, with a contribution of ~70%. Secondary contributors were sliding speed (~14%), and load and steel hardness (~12%). Following the wear tests, residual stress measurements were conducted on polymer reinforced with carbon fibre. It was found that compressive residual stresses existed, and that their magnitude increased with increasing load.

Keywords: Polymer, PEEK, Steel, Wear

1. Introduction

The Oil & Gas industry involves extreme temperatures, pressures and chemical environment that demands precision engineering equipment. Due to this aggressive environment sealing components are always at great risk of failure meaning that special attention to seal's material is requested. T-seals are made of thermoplastic and commonly used in radial applications, for instance around the outside of a piston to prevent the tendency to rotate under motion, avoiding typical spiral failure under extreme conditions.
The properties of polymers can be improved with incorporation of reinforcements into the polymer matrix. Much of the research has focused on how the properties of the resulting polymer composites depend on factors such as reinforcement material, concentration and even orientation within the matrix material [1].

Due to growing industrial popularity of polymer composites, there is a need to investigate how the inclusion of reinforcements to polymers affects tribological performance. A variety of researchers have focused their efforts in analysing the wear experienced by reinforced polymer-steel sliding pairs. The wear experienced between several polymers against the same steel surface using Pin on Disk equipment has been investigated. These researchers reported that the behaviour of polymers under wear does not follow the typical patterns expected from metal against metal, as each polymer behaves in a unique way depending on composition and reinforcement type [2].

The friction and wear behaviour of Polyether Ether Ketone (PEEK) and its carbon fibre reinforced composites under dry sliding against steel has been studied. The findings showed that the inclusion of short carbon fibres improved the wear resistance of PEEK and reduced the Coefficient of Friction (CoF). It was also noted that the inclusion of 10 vol.% carbon fibres provided an optimal level of reinforcement with the biggest reduction in specific wear being experienced (from 10^{-5} mm^3/Nm at 0% to $0.02x10^{-5}$ mm^3/Nm at 10%) [3].
In 2006 the wear behavior of PEEK and its composites against steel in dry sliding conditions was investigated [4]. The statistical analysis of the influence of load, temperature and sliding distance on wear of PEEK-CF30 found that increasing temperature and sliding distance lead to a significant increase in weight loss. Later on the research focused on the effect of reinforcement (Glass fibre and Carbon fibre) on friction and wear [5]. Overall these results [4-5] demonstrated that for a Steel/PEEK pairing the reinforcement of PEEK with glass fibres (GF-PEEK) or PEEK with carbon fibres (CF-PEEK) lead to a significant reduction in the specific wear rate. Specific wear rates for PEEK and carbon reinforced PEEK (CF30-PEEK, referred as PEEK reinforced with CF30 wt.%) saw the biggest reduction of ~90% from $9.08x10^{-6}$ mm^3/Nm to 0.847×10^{-6} mm^3/Nm.
The friction and wear behavior of PEEK and CF-PEEK against 316L stainless steel with seawater lubrication has been compared [6]. The worn surfaces of the PEEK and CF-PEEK specimens were observed by a microscope. It was found that the 316L/PEEK pair resulted in a much rougher surface with a lot of grooves and scratches compared to the 316L/CF-PEEK pair resulting in a smoother and flatter surface. It was concluded that inclusion of carbon fibres had greatly improved the friction mechanism and therefore wear performance [6].

It was also determined that CoF is most influenced by sliding distance, alongside temperature [4]. Li et al. [7], studied the effect of reinforcing PEEK with glass fibres, where a higher CoF across the entire sliding distance was observed, yet the GF-PEEK had the greatest wear resistance when compared to virgin PEEK.
Residual stresses have a direct influence on an engineering component's performance in service; the influence can be either beneficial or detrimental depending on the type and magnitude of the stress. Through many general investigations it has been shown that compressive residual stresses at the surface are usually beneficial to fatigue life [8-10].

Knowledge on how tribological loading affects residual stresses is essential to help predict how they may evolve during the lifetime of a component.
LeMaster et al. [11], investigated the resulting stresses from a finishing grinding process. The initial residual stresses due to manufacturing processes were measured alongside measuring the residual stresses in the material post-grinding. Results showed that a fairly uniform and constant compressive residual stress field existed both before and after grinding, but that grinding reduced the average residual stress. A linear relationship between the changes in residual stress and the grinding depth was developed.
The influence of pre-existing residual stresses on the wear behaviour of steels, with a metal to metal sliding pair has been studied, where it was concluded that the changes in residual stresses due to wear are independent of the initial stress distribution, unless the initial stress pattern involves values larger than those produced by wear [12].

Vanarotti et al. conducted a study showing that wear testing of metal matrix composites caused the generation of residual stresses. It was indicated that these compressive residual stresses after wear testing were the result of the internal permanent strains generated during wear [13].

To further existing research, a comprehensive Taguchi-based experimental plan, varying several parameters was conducted to demonstrate the relative effects of reinforcement concentration and reinforcement type on specific wear rate. This specific wear rate study will present new findings by identifying the optimal combination of normal load, sliding speed, disk hardness and pin reinforcement. In addition to the study of wear an analysis of residual stresses experienced between the particular steel-polymer sliding pair combinations will be investigated. This combination has been chosen to simulate the wear experienced between a polymer anti-extrusion ring and a steel sealing surface. These replaceable rings are commonly used to prevent metal-to-metal contact of moving parts in sealing geometries to help prolong equipment life [14].

From the authors' knowledge, the analysis of residual stresses post wear testing of a polymer-steel sliding pair has not been researched before. A new contribution in knowledge will be presented by analysing the residual stresses post wear testing. Experimentation with a polymer-steel sliding pair and varying load will be conducted, as well as the residual stresses in the steel measured using X-Ray Diffraction (XRD). Comparing the nature of the residual stresses will allow identify a relationship between loading during wear testing and resulting residual stress.

2. Materials and Methods

2.1 Material Characteristics

2.1.1 Tool Steel - Disk

Twelve disk, of 75mm diameter and 3mm thickness were cut from a ground flat tool steel plate provided by MSC Industry.

Table 1 shows the chemical composition of the steel disk recorded using Glow Discharge Optical Emission Spectrometry model Horiba GD-OES profilometer following ISO 14707 (2015) standard [15].

Table 1 Chemical Composition of the Steel Disk

Element	C	Mn	W	Cr	V	Si
wt. % (±0.01)	1.05	1.23	0.46	0.58	0.27	0.28

To produce steel disks with a range of hardness values, heat treatments were undertaken following the information provided by the steel supplier [16]. The twelve disks were divided into three groups of four. Group 1 was untreated, while Groups 2 and 3 were subjected to different heat treatments to modify their hardness. The samples were placed in a furnace at 600℃, the temperature raised to 800℃ where samples were held for 8 minutes (soak time for a material is dependent on the thickness). Both groups (2 and 3) were then oil quenched. Post quenching samples were tempered for one hour, Group 2 at 200℃ and Group 3 at 350℃.

Following heat treatments, the samples were metallographic prepared using a Struers rotopol 21 following the Guide for Preparation of Metallographic Specimens ASTM E3-01 [17]. Figures 1a and 1b show images of the grain structure for each of the groups. A microstructure with spherical carbides can be observed for both of the treated sample with Figure 1a showing a ferrite matrix (Group 1).

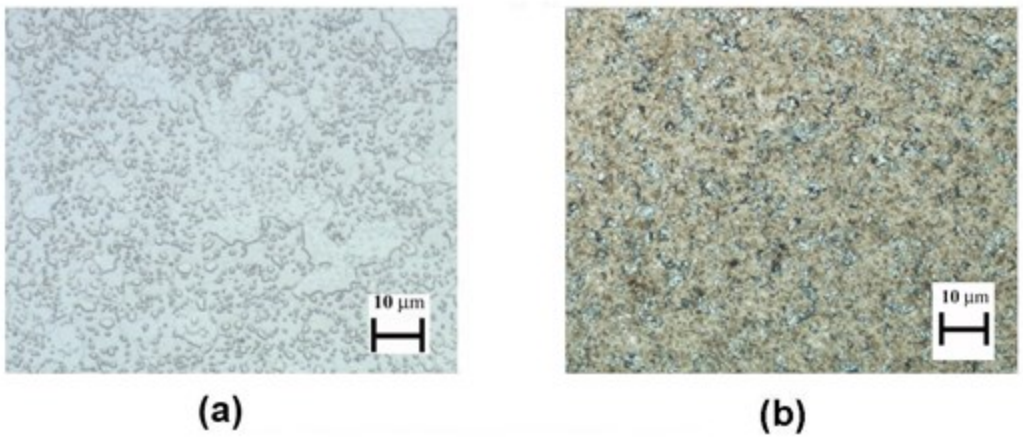

Figure 1 Metallographic Study of Steel Disks (a) Untreated - Group 1
(b) Treated - Groups 2 & 3

Hardness tests for all of the samples were conducted using a Mitutoyo MVK G1 microhardness tester according to the standard test method for Vickers Hardness of Metallic Materials, ASTM E92-82 [18]. In this case a 5kg load diamond indenter was pressed into the steel for 15 seconds. The Vickers hardness for each of the groups is shown in Table 2.

Table 2 Hardness of Heat Treated Steel Disks

Steel Disks	Hardness (HV)
Group 1	211
Group 2	699
Group 3	630

2.1.2 PEEK - Pin

Polyether Ether Ketone (PEEK) injected molded to a diameter of 6.5 mm with different reinforcement materials (carbon fibres or glass fibres) and different weight concentration of reinforcement (0wt.% reinforcement, 20wt.% carbon, 30wt.% carbon and 30wt.% glass) were provided by Victrex to be used as the pin material. These reinforcements are widely used and main reason for testing and searching for optimal wear conditions. The pins were machined to a length of 28mm, to fit the Pin on Disk Tribometer.

Table 3 lists the grades of PEEK chosen and their material properties of interest.

Table 3 Material Properties of interest for grades Polyether Ether Ketone (PEEK)

Grade of PEEK	Reinforcement (wt. %)	Density, ρ (g/cm^3)	Glass Transition Temp, T_g	Melting Temp, T_m	Polymer Hardness, Shore D
450G	0%	1.30	143˚C	343˚C	84.5
450CA20	20% Carbon	1.37	143˚C	343˚C	86.0
450CA30	30% Carbon	1.40	143˚C	343˚C	87.5
450GL30	30% Glass	1.51	143˚C	343˚C	87.5

A four digit code (XXYY) was established to identify different reinforced PEEK.
XX: type of fibre (CF: Carbon fibre, GF glass fibre)
YY: wt.% (20 or 30).
e.g. CF20-PEEK indicates PEEK reinforced with 20wt.% Carbon Fibre

2.2 Wear Test Experimental conditions

2.2.1 Equipment

Experiments were carried out using a Pin on Disk Tribometer with dry sliding conditions. Further details for the Pin on Disk testing method can be found in the ASTM G99-04 international standard for tribotesting [19].
The measurement of wear method adopted for this research is based on a change in mass which is then equated to a change in volume. The mass of the pin before and after each trial was measured using a Mettler Toledo, MS204/M analytical balance, which has Maximum Capacity 220g and readability 0.0001g.

2.2.2 Wear Parameters

Normal load, sliding speed, disk hardness and pin reinforcement are the parameters of interest for this study. The sliding distance was kept constant for all tests at 10km. This value for sliding distance was chosen based on previous research [5], showing that for the experiments carried out on carbon and glass reinforced PEEK a minimum sliding distance of 5km was required to reach a steady state Coefficient of Friction (CoF).

Tables 4 and 5 show the test parameters and levels required to investigate their influence on wear. As mentioned, the objective of this study is to investigate the influence of carbon reinforcement wt.% and type of reinforcement material on wear and residual stresses. Table 4 details the carbon reinforcement wt.% chosen. Table 5 details the various reinforcement materials chosen.

Table 4 Experimental parameter levels selected to study the influence of carbon wt.% on the wear analysis

Level	Load (N)	Speed (m/s)	Disk Hardness (HV)	Pin reinforcement (wt.%)
1	10	1.0	Group 1 (211)	0
2	20	1.2	Group 2 (699)	20
3	30	1.4	Group 3 (630)	30

Table 5 Experimental parameter levels selected to study the influence of type of reinforcement material on the wear analysis with 30 wt.% of reinforcement.

Level	Load (N)	Speed (m/s)	Disk Hardness (HV)	Pin Reinforcement Material
1	10	1.0	Group 1 (211)	Virgin

2	20	1.2	Group 2 (699)	Carbon
3	30	1.4	Group 3 (630)	Glass

2.2.3 Wear Experiments

A comparison study was carried out to investigate whether type of reinforcement material or wt.% has a larger influence on wear and furthermore on the residual stress. The experimental method required two L9 orthogonal arrays. The two arrays are further referred to Orthogonal Array 1 and Orthogonal Array 2, where they represent carbon reinforcement percentage and type of reinforcement material respectively. Tables 6 and 7 show the run order generated by the L9 orthogonal arrays selected for the study.

Table 6 L9 Orthogonal Array 1 – Investigation of the influence of carbon reinforcement wt.% on wear of PEEK when in contact with tool steel disks with different hardness.

Trial	**Parameter**			
	F_N **(N)**	v **(m/s)**	**Hardness (HV)**	**Carbon Reinforcement wt.%**
1	10	1.0	Group 1 (211)	0
2	10	1.2	Group 2 (699)	20
3	10	1.4	Group 3 (630)	30
4	20	1.0	Group 2 (699)	30
5	20	1.2	Group 3 (630)	0
6	20	1.4	Group 1 (211)	20
7	30	1.0	Group 3 (630)	20
8	30	1.2	Group 1 (211)	30
9	30	1.4	Group 2 (699)	0

Table 7 L9 Orthogonal Array 2 – Investigation of the influence of type of reinforcement material on wear of PEEK (30 wt.%) when in contact with tool steel disks with different hardness.

Trial	Parameter			
	F_N (N)	v (m/s)	Hardness (HV)	Reinforcement Material
1	10	1.0	Group 1 (211)	Virgin
2	10	1.2	Group 2 (699)	Glass
3	10	1.4	Group 3 (630)	Carbon
4	20	1.0	Group 2 (699)	Carbon
5	20	1.2	Group 3 (630)	Virgin
6	20	1.4	Group 1 (211)	Glass
7	30	1.0	Group 3 (630)	Glass
8	30	1.2	Group 1 (211)	Carbon
9	30	1.4	Group 2 (699)	Virgin

2.3. Analysis of Variance (ANOVA)

Analysis of variance is a collection of statistical models used to compare the means of more than two populations and the variance in their associated procedures. This allows a visual of the contribution of each of the variables to the specified performance parameter to be obtained.

2.3.1. Signal-To-Noise ratio (S/N)

The S/N ratio served as the objective function for optimization required to carry out ANOVA. It is a measure used to compare the level of a desired signal to the level of background noise; it is often expressed in decibels. There are three different forms of the S/N ratio that are of common interest for the optimization of static problems: i) Smaller-the-better, ii) Larger-the-better and iii) Nominal-the better.

Since the response for the model is wear rate, to enhance tribological performance it is desired to achieve the lowest wear rate hence the signal to noise ratio of interest is "the smaller-the-better". The S/N ratio for this case is a logarithmic transformation of the wear rate. Equation 1 shows how to calculate "smaller-the-better" S/N ratio, where W_s is the specific wear rate and n is the number of observations [20].

$$S/N = -10 \log\left[\frac{1}{n}\left(\sum {W_s}^2\right)\right] \quad (1)$$

2.4. PARETO Chart

Pareto's charts are used to illustrate the contribution of each variable, in this case information obtained through ANOVA analysis. For this purpose, Excel Microsoft spreadsheet can be used where bars in descending order for each individual values and the cumulative total is provided.

2.5 Residual Stress Measurement conditions

2.5.1 Equipment

Residual stress measurements were carried out using X-Ray Diffraction (XRD) with the BRUKER D8 advance XRD. Further details for the experimental procedure can be found in the National Physical Laboratory Measurement Good Practice Guide No. 52 [21].
Kα radiation from a Chromium X-ray was used, as recommended by the procedure for an Iron-based alloy [22, 23]. As recommended by the literature the method used to determine the stress is, $\sin^2 \varphi$ with Pearson 7 [22, 23].

2.5.2 Residual Stress Measurements

For the residual stress measurement, three additional wear experiments were conducted at different loads (10N, 20N and 30N) to allow the author to investigate the possibility of a relationship between loading during wear testing and residual stress formation. A constant sliding speed (1.0m/s), sliding distance (10km), and tool steel disk hardness (Group 1, 211HV) were selected. These constant parameter levels were specifically chosen to reduce the presence of unnecessary residual stresses. A sliding speed of 1.0m/s produces less vibration during the experiments and the sliding distance of 10km will ensure a stable CoF, as reported in previous research [5].

After the wear test, residual stress measurements were taken at two points on the disks. The first point to measure was taken in the parent material to account for residual stresses occurring due to manufacturing processes of the bar where the disks were cut from, and the second point to measure was taken in the wear track developed during the wear test. Computing the difference between these two measurements provided an estimate for the effect that the wear test has on the residual stress.

3. Results and Discussion

Table 8 show a summary for all results measured and calculated, relevant to wear testing. Specific wear rate, W_s was calculated using Equation 2.

$$W_s = \frac{\Delta V}{F_N L} \tag{2}$$

Where:
ΔV: Change in volume (mm^3)
F_N: Normal load (N)
L: Sliding distance (m)

Table 8 Summary of all recorded results such as mass loss and specific wear rate for each trial

Trial	F_N (N)	v (m/s)	Hardness (HV)	Pin Material	Mass Loss Pin (g)	W_s (x10^{-6} mm^3/Nm)
1	10	1.0	Group 1 (211)	PEEK	0.0010	7.96
2	10	1.2	Group 2 (699)	CF20-PEEK	0.0003	2.19
3	10	1.4	Group 3 (630)	CF30-PEEK	0.0005	3.57
4	20	1.0	Group 2 (699)	CF30-PEEK	0.0009	3.21
5	20	1.2	Group 3 (630)	PEEK	0.0027	10.38
6	20	1.4	Group 1 (211)	CF20-PEEK	0.0018	6.57
7	30	1.0	Group 3 (630)	CF20-PEEK	0.0011	2.68
8	30	1.2	Group 1 (211)	CF30-PEEK	0.0015	3.57
9	30	1.4	Group 2 (699)	PEEK	0.0052	13.33
10	10	1.2	Group 2 (699)	PEEK	0.0017	11.26
11	20	1.4	Group 1 (211)	GF20-PEEK	0.0026	8.61
12	30	1.0	Group 3 (630)	GF30-PEEK	0.0022	4.86

From the results shown in Table 8 it can be seen that the specific wear rate for all trials ranged from 2.19 x10^{-6} to 13.33 x10^{-6} mm^3/Nm. The specific wear rate results shown here can be compared to the specific wear rate experienced in the research for PEEK against steel in long dry sliding condition [6]. Other researchers [5] reported that for varying levels of reinforced PEEK at a constant 15km sliding distance the specific wear rate ranged from 0.61 x 10^{-6} to 9.08 x 10^{-6} mm^3/Nm depending on the severity of the parameters.

Figures 2a and 2b show images of unworn and worn surfaces of the steel disk, respectively.

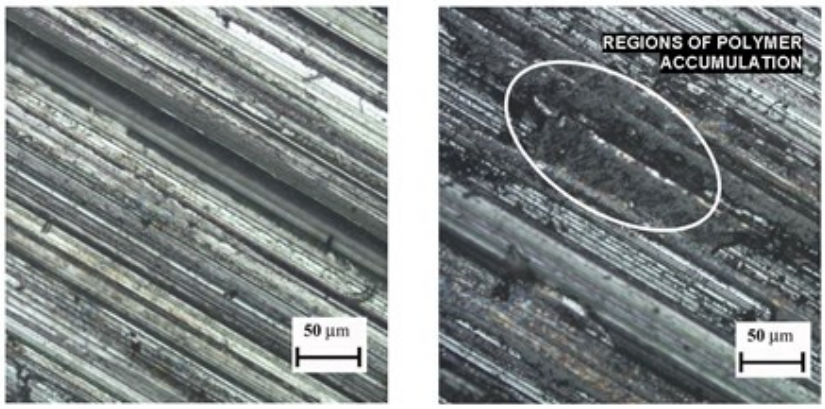

Figure 2 Steel disk surface (a) Unworn, machined surface (b) Worn surface showing PEEK accumulation

Inspection of Figure 2b reveals that there has been very little deformation on the surface of the steel, but rather some of the pin's material has been deposited onto the steel's surface. This depositing of polymer to the surface of the steel agrees with research

conducted by [13], where microscopy images of the worn steel surface showed debris accumulation.

3.2 Analysis of the wear

3.2.1 Wear on Surface of the PEEK - Pin

Visual inspection of worn pins showed that they were much smoother due to loss of material. A study of the pins was conducted by gold coating an unworn pin and one which had undergone extreme wear conditions for the various pin reinforcements. The surfaces of each of these pins were examined using a Hitachi S-3700 N Scanning Electron Microscope (SEM). Figures 3a to 3d show a summary of the typical surfaces for virgin and CF-PEEK pins.

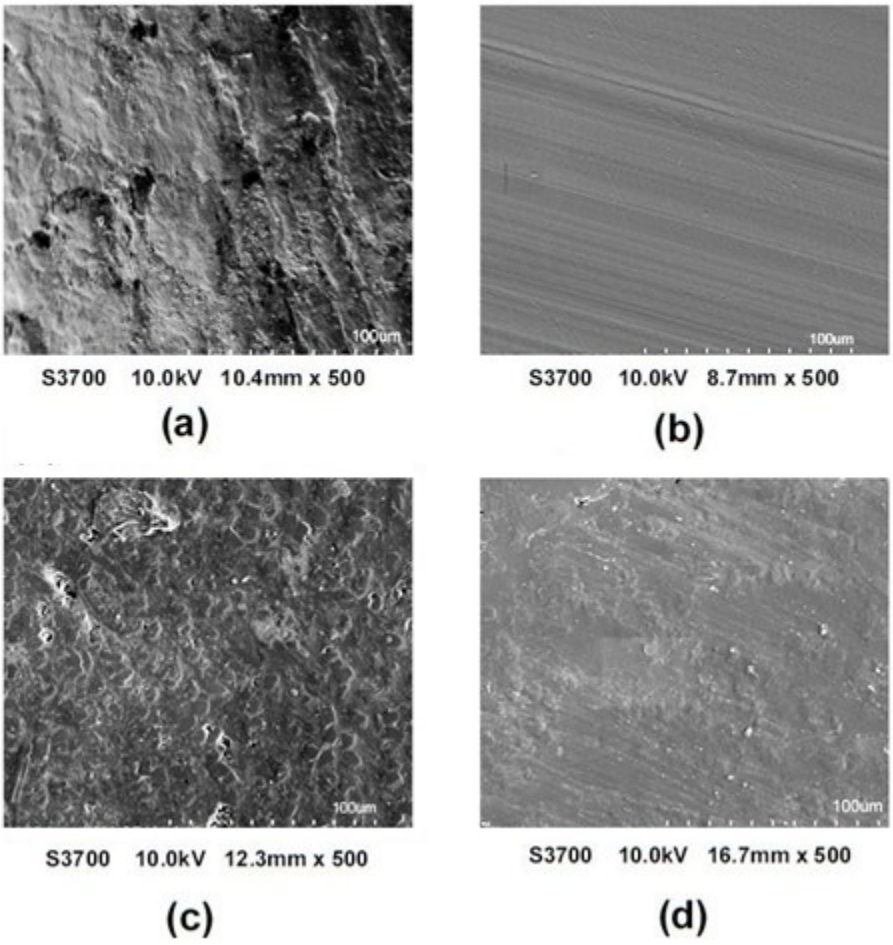

Figure 3 SEM study of PEEK pins (a) Unworn – Virgin pin (b) Worn – Virgin pin (c) Unworn –CF20-PEEK (d) Worn – CF20-PEEK

As observed in Figure 3b and 3d; various degrees of wear tracks, in the direction of sliding, have formed over the surface of the worn pins. The prominence of the wear tracks observed on the surface of the pin was found to be dependent on the severity of the wear experienced. The formation of wear tracks on the surface of the worn reinforced pins was inhibited by the fibres, similar phenomenon has been documented by other

researchers [5, 7 and 24]. One common explanation is that material removal close to the fibres was interrupted thus causing an accumulation of wear debris around them.

3.3 Influence of Selected parameters on specific wear rate

Main effect plots have been created to show the relative effect of each level of the parameters on specific wear rate. Since two L9 orthogonal arrays have been used, two sets of main effects plots have been created and superimposed on each other. To create the plots, mean values for each level of parameter needed to be calculated, Table 9 shows these results.

Table 9 Mean response for Specific Wear Rate

Wear Parameters		Mean Specific Wear Rate (x10^{-6} mm^3/Nm)		
		Level 1	**Level 2**	**Level 3**
Orthogonal Array 1	F_N (N)	4.57	6.72	6.53
	v (m/s)	4.62	5.38	7.82
	Hardness (HV)	6.03	6.24	5.54
	Reinforcement (%)	10.56	3.81	3.45
Orthogonal Array 2	F_N (N)	7.60	7.40	7.25
	v (m/s)	5.34	8.40	8.50
	Hardness (HV)	6.71	9.27	6.27
	Reinforcement Material	10.56	8.42	3.45

Note: refer to Table 5 for each level information

3.3.1 Influence of Load, Speed & Hardness on Specific wear rate

Figures 4a to 4c show the influence of load, sliding speed and tool steel disk hardness on the specific wear when varying the reinforcement wt.% and reinforcement material.

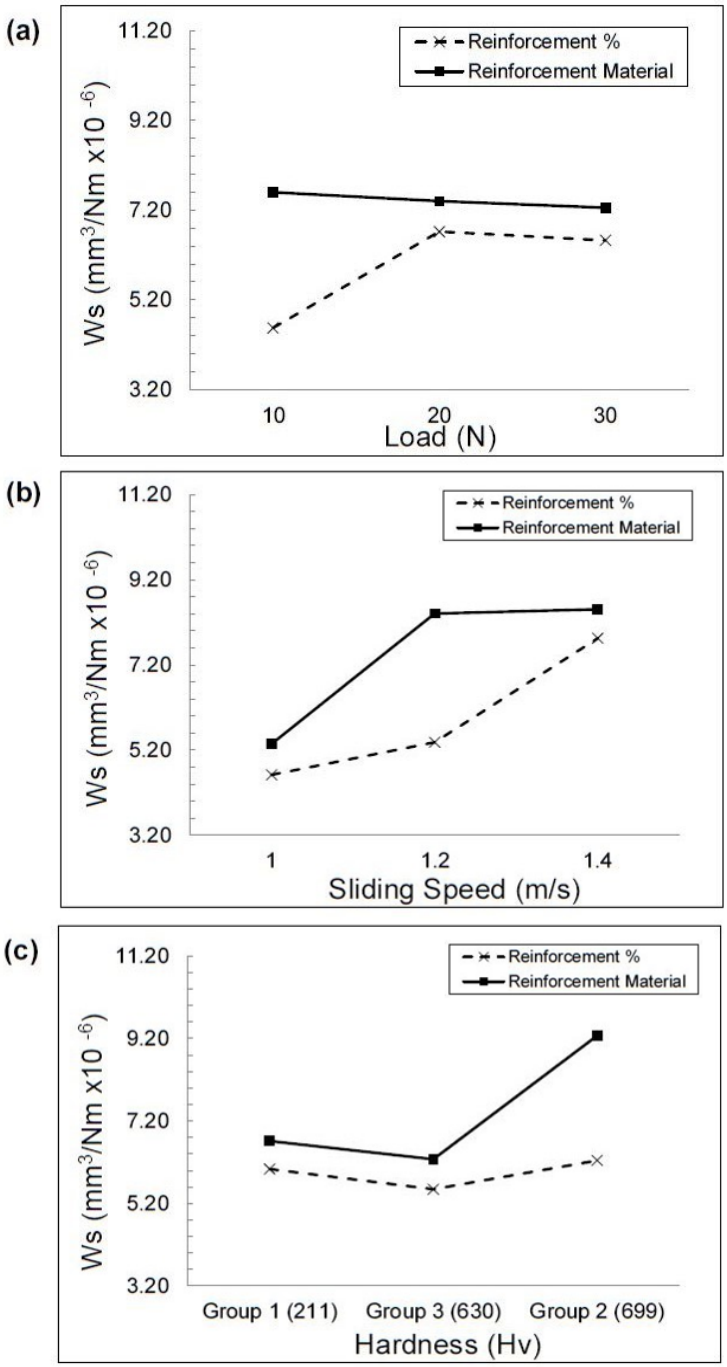

Figure 4 Variation in Specific Wear Rate for reinforced percentage and type of reinforced material (a) Load (b) Sliding Speed (c) tool steel Disk Hardness

Figure 4 shows in general how wear rate is affected when reinforcing a sample (independently on the type of reinforced material) and when sample is reinforced independently of wt.% value. Figure 4a shows that in general an increase in load causes a slight decrease in specific wear rate particularly at the higher load levels (greater than 20N). However, there is an anomalous result when studying the influence of the carbon

wt.% at loads <20N, where an increase of 100% in the load (from 10N to 20N) produced an increase in specific wear rate of 48% (from 4.57 $x10^{-6}$ to 6.72 $x10^{-6}$ mm^3/Nm). When using loads >20N a decrease in average specific wear rate by 3% (from 7.40 $x10^{-6}$ to 7.15 $x10^{-6}$ mm^3/Nm) was observed. The small changes seen here are in line with results shown by [2], who concluded that an increase in contact pressure had no much influence in average specific wear rate.

Figure 4b shows that in general an increase in sliding speed produced an increase to the specific wear rate. These results are in agreement with previous results [2], who suggested that an increasing speed caused a rise in temperature towards the softening point of the polymer, which lead to higher levels of adhesion thus increasing the specific wear rate. Additionally, it can be seen that the type of reinforcement material has a higher impact on specific wear rate compared to wt.% reinforcement. It is observed that an increase of specific wear rate by 57% (from 5.34 $x10^{-6}$ to 8.40 $x10^{-6}$ mm^3/Nm) is observed independently on type of reinforced material, compared to an increase of specific wear rate by ~16% (from 4.62 $x10^{-6}$ to 5.38 $x10^{-6}$ mm^3/Nm) when wt.% is varied.

Figure 4c shows the influence of tool steel hardness on the specific wear rate. As observed, the results of this graph are inconclusive; as in general hardness <630 HV produced a decrease in specific wear rate of ~8% (from 6.03 $x10^{-6}$ to 5.54 $x10^{-6}$ mm^3/Nm and from 6.71 $x10^{-6}$ to 6.27 $x10^{-6}$ mm^3/Nm). However, a further increase in disk hardness >630HV produced an increase of the specific wear rate by ~13% (from 5.54 $x10^{-6}$ to 6.24 $x10^{-6}$ mm^3/Nm) for carbon percent and by 48% (from 6.27 $x10^{-6}$ to 9.27 $x10^{-6}mm^3$/Nm $x10^{-6}$) for reinforced materials. In general, [24] found that for various levels of hardened specimens the wear rates increased non-linearly.

3.3.2 Influence of Polymer Reinforcement on Specific Wear Rate

Figures 5a and 5b show the influence of carbon wt.% reinforcement and in general type of reinforcement material on the specific wear rate.

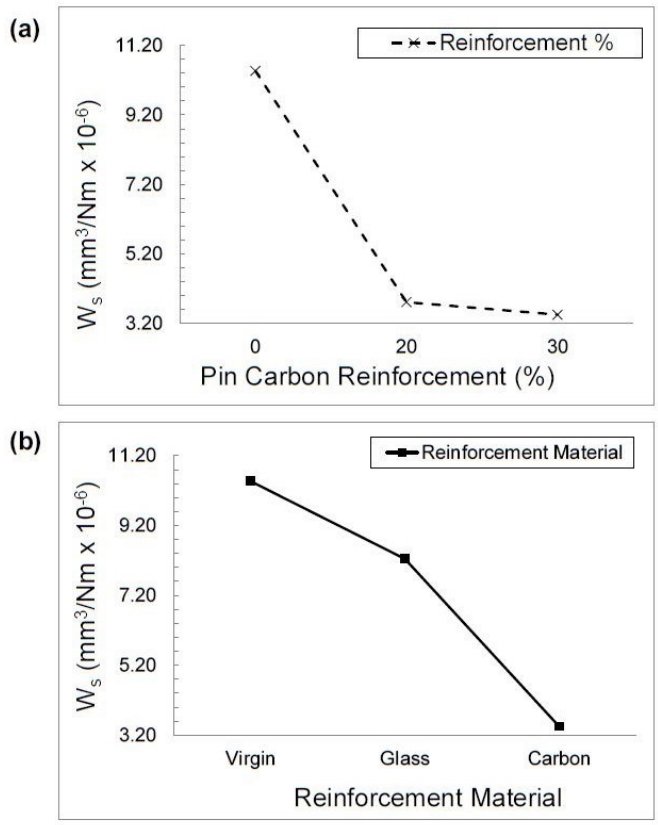

Figure 5 Variation in Specific Wear Rate for (a) Increasing pin carbon reinforcement concentration (b) Varying pin's type of reinforcement material at a constant reinforcement concentration

Figure 5a shows that as the carbon wt.% reinforcement is increased the specific wear rate decreased. It can be seen however that after the initial inclusion of carbon wt.% reinforcement the reduction in specific wear rate is of a much smaller magnitude suggesting that there is an optimum level of inclusion. The initial increase in carbon wt. % reinforcement in 20% showed a decrease in specific wear rate by 64% (from 10.56 $x10^{-6}$ to 3.81 $x10^{-6}$ mm^3/Nm) whereas for reinforcement >20% a decrease in 9% of the specific wear rate (from 3.81 $x10^{-6}$ to 3.45 $x10^{-6}$ mm^3/Nm) was observed. Despite using vol% in previous research a similar effect when investigating the inclusion of carbon reinforcement to PEEK was observed [3], where it was concluded that by increasing the carbon percentage the specific wear rate decreased by one order of magnitude, but that above 10 vol.% fibre content only a slight improvement was seen. The decrease in wear rate in reinforced PEEK can be related to the fact that the hardness of the pin has been enhanced and according to the Archard Equation which is based on asperity contacts and describes sliding wear as the hardness increases wear rate decreases [25]

Figure 5b also shows that the specific wear rate greatly decreased with the inclusion of reinforcement material. GF30-PEEK produced a decreased of 26% on the specific wear rate (from 10.56 $x10^{-6}$ to 8.42 $x10^{-6}$ mm^3/Nm). This relationship is in agreement with results showing that the inclusion of reinforcement to the PEEK reduced the specific

wear rate and that the magnitude of this effect was dependent on type of reinforcement material [5].

3.4 Analysis of the Variance (ANOVA)

Analysis of variance has been carried out to allow an even more detailed look at how each parameter contributes towards the wear by producing an estimate for the percentage contribution of each parameter. The S/N ratio of interest is "the smaller the better," calculated using Equation 1. The calculated S/N values can be seen in Table 10.

Table 10 Summary of all recorded results for each trial and the calculated S/N ratio

Trial	Load (N)	Speed (m/s)	Disk Hardness (HV)	Pin Reinforcement Percentage Carbon (%)	Mass Loss Pin (g)	S/N Ratio (dB)
1	10	1.0	Group 1 (211)	0	0.0010	102.28
2	10	1.2	Group 2 (699)	20	0.0003	113.19
3	10	1.4	Group 3 (630)	30	0.0005	108.94
4	20	1.0	Group 2 (699)	30	0.0009	109.86
5	20	1.2	Group 3 (630)	0	0.0027	99.67
6	20	1.4	Group 1 (211)	20	0.0018	103.65
7	30	1.0	Group 3 (630)	20	0.0011	111.45
8	30	1.2	Group 1 (211)	30	0.0015	108.94
9	30	1.4	Group 2 (699)	0	0.0052	97.50
				Material Type		
10	10	1.2	Group 2 (699)	Glass	0.0017	98.97
11	20	1.4	Group 1 (211)	Glass	0.0026	101.30
12	30	1.0	Group 3 (630)	Glass	0.0022	106.27

3.4.1 Summary of ANOVA results for influence of carbon reinforcement percentage

ANOVA was carried out for the carbon wt.% reinforcement trials, Orthogonal Array 1 Figure 6 shows the percentage contribution for each of the experimental parameters with respect to specific wear rate considering the percentage of carbon reinforcement.

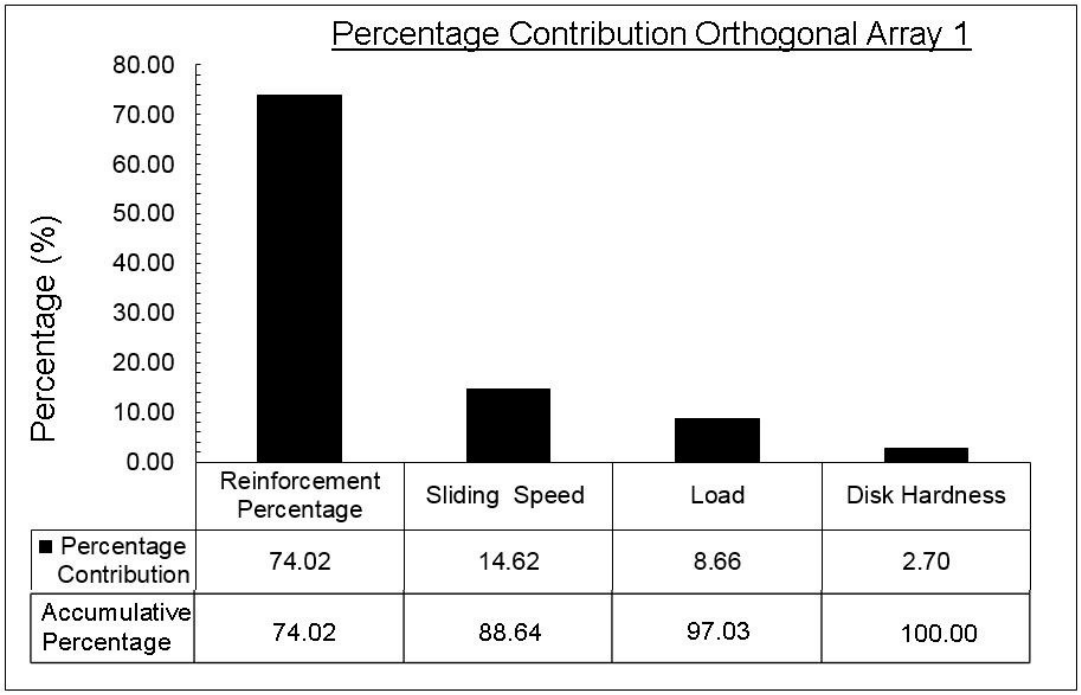

Figure 6 Pareto Chart for ANOVA for specific wear rate considering the percentage carbon reinforcement

From Figure 6 it can be seen that the primary contribution to the specific wear rate is from wt.% reinforcement, with a contribution of ~74%. Secondary contributors are sliding speed and load with ~23%. The disk hardness has almost insignificant effects (3%) on the specific wear rate when compared to the wt.% reinforcement influence.

3.4.2 Validation of Optimal Parameters for Orthogonal Array 1

The optimum level of each parameter was identified by plotting the S/N ratio, the highest S/N ratio corresponds to the optimal parameter, which in this case provides the smallest mass loss and as a consequence the smallest wear rate, Figure 7. To achieve the smallest mass loss for these trials the optimum levels for the parameters are A1B1C2D2 (Load 10N, sliding speed 1.0m/s, Group 2 disk hardness 699HV and 20 wt.% carbon reinforcement).

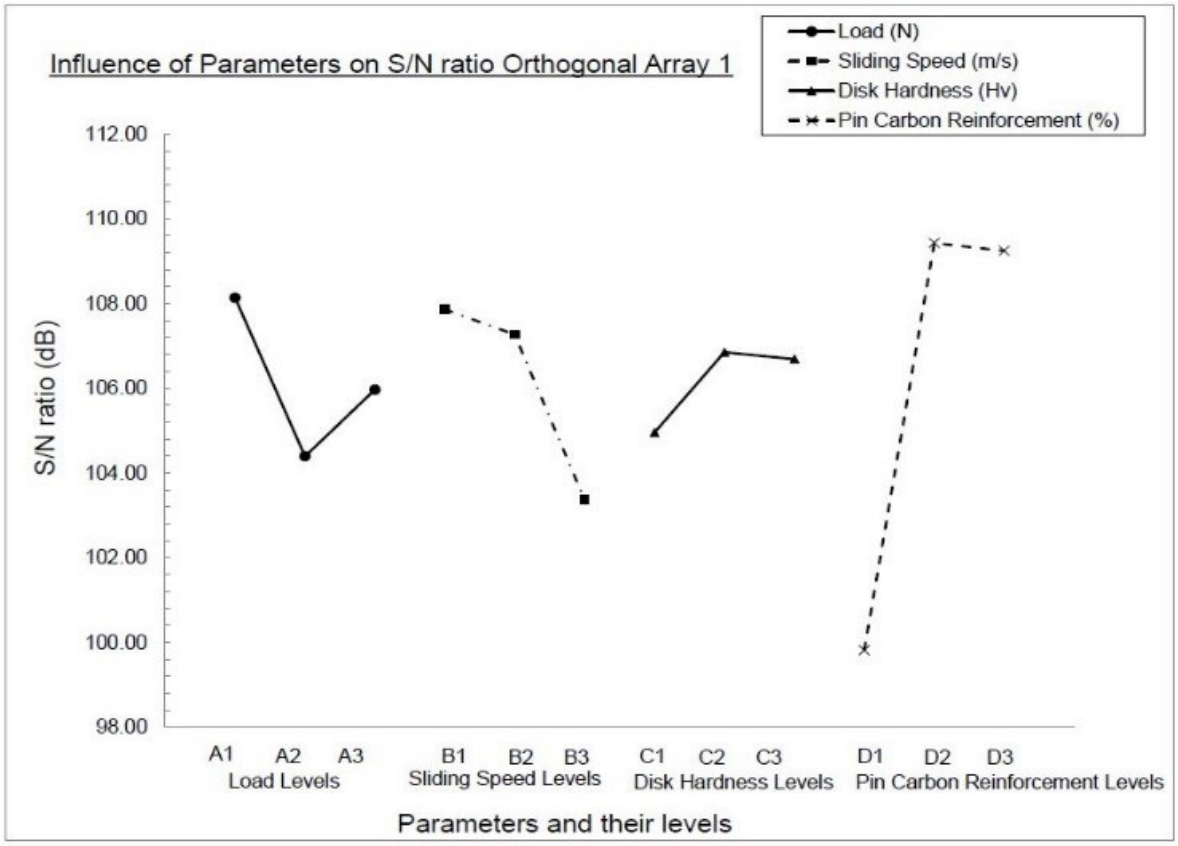

Figure 7 Mean S/N ratio for all parameters and levels for low mass loss considering wt.% Carbon Reinforcement

An estimated S/N ratio (η') based on optimal parameters can be calculated using Equation 3, where η_m represents an average of the mean S/N ratio for all trials, and η_{im} represents the mean S/N ratio for the optimum parameters. The results from the confirmation experiments were averaged and compared with the predicted average, Table 11.

$$\eta' = \eta_m + \sum_{i=1}^{o} (\eta_{im} - \eta_m) \tag{3}$$

Table 11 Results of mass loss based on carbon reinforcement percentage– Orthogonal Array 1

	Optimal Parameters	
	Prediction	**Experiment**
S/N Ratio (dB)	110.52	110.69
Mass Loss (g)	0.0004	0.0004

As can be seen from Table 11 the predicted results were very accurate as they were very close to the actual experimental results.

3.4.3 Summary of ANOVA results for Different Types of Reinforcement Material

ANOVA was carried out for the type of reinforcement material trials, Orthogonal Array 2. Figure 8 shows the percentage contribution for each of the experimental parameters with respect to specific wear rate considering type of reinforcement material (constant 30 wt.% reinforcement)

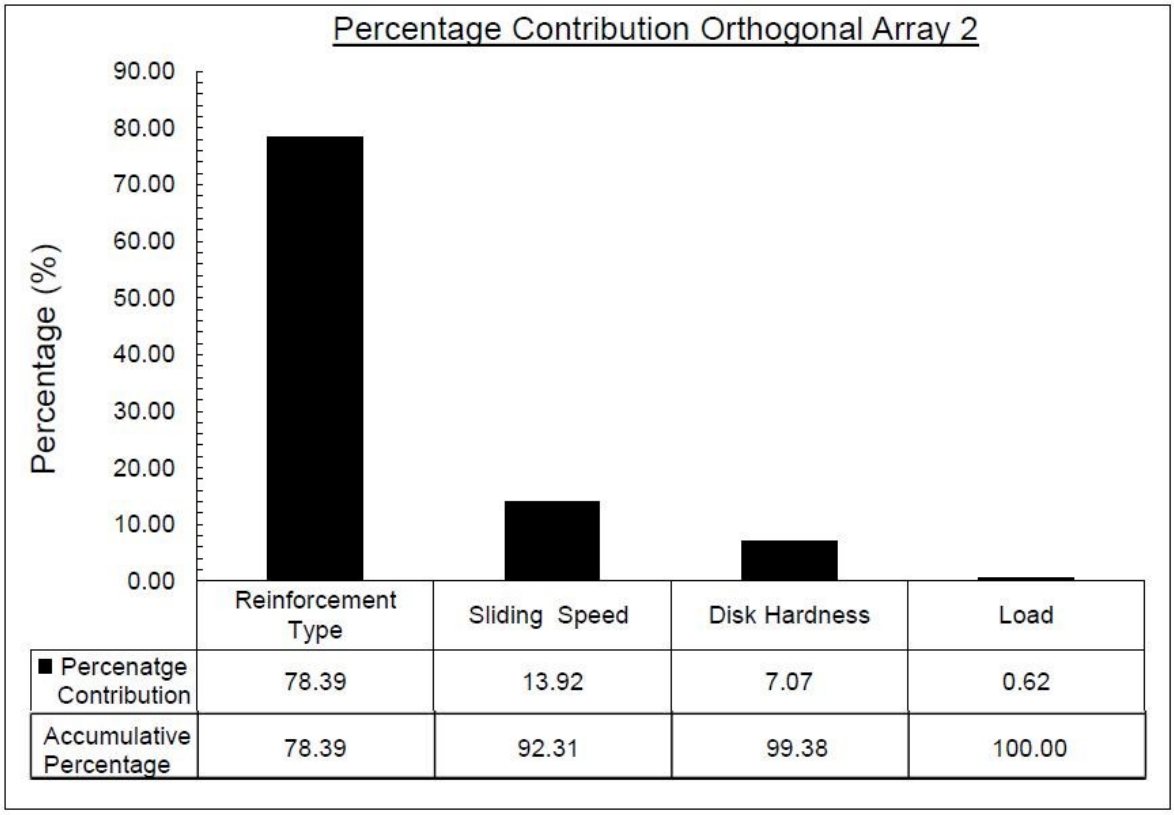

	Reinforcement Type	Sliding Speed	Disk Hardness	Load
Percenatge Contribution	78.39	13.92	7.07	0.62
Accumulative Percentage	78.39	92.31	99.38	100.00

Figure 8 Pareto Chart for ANOVA for specific wear rate based on type of reinforced material for 30wt.% reinforcement

From Figure 8 it can be seen that the primary contribution to the specific wear rate is from reinforcement material type, with a contribution of ~78%. Secondary contributors are Sliding speed and load with ~13% and 7% respectively. The disk hardness has almost insignificant effects (<1%) on the specific wear rate when compared to the reinforcement influence. These results mirror those seen above for wt.% carbon reinforcement trials.
Comparing both sets of ANOVA results for the two orthogonal arrays shows that wt.% carbon reinforcement and type of reinforcement material have a similar influence over mass loss experienced, with both of the variables showing a percentage contribution in the range of 70%.

3.4.4 Validation of Optimal Parameters for different types of Reinforced Material

The S/N ratio for these trials was plotted, again the highest S/N ratio corresponds to the optimal parameter, Figure 9. To achieve the smallest mass loss the optimum levels for the parameters are A3B1C3D3 (Load 30N, sliding speed 1.0m/s, Group 3 disk hardness 630HV and glass reinforcement)

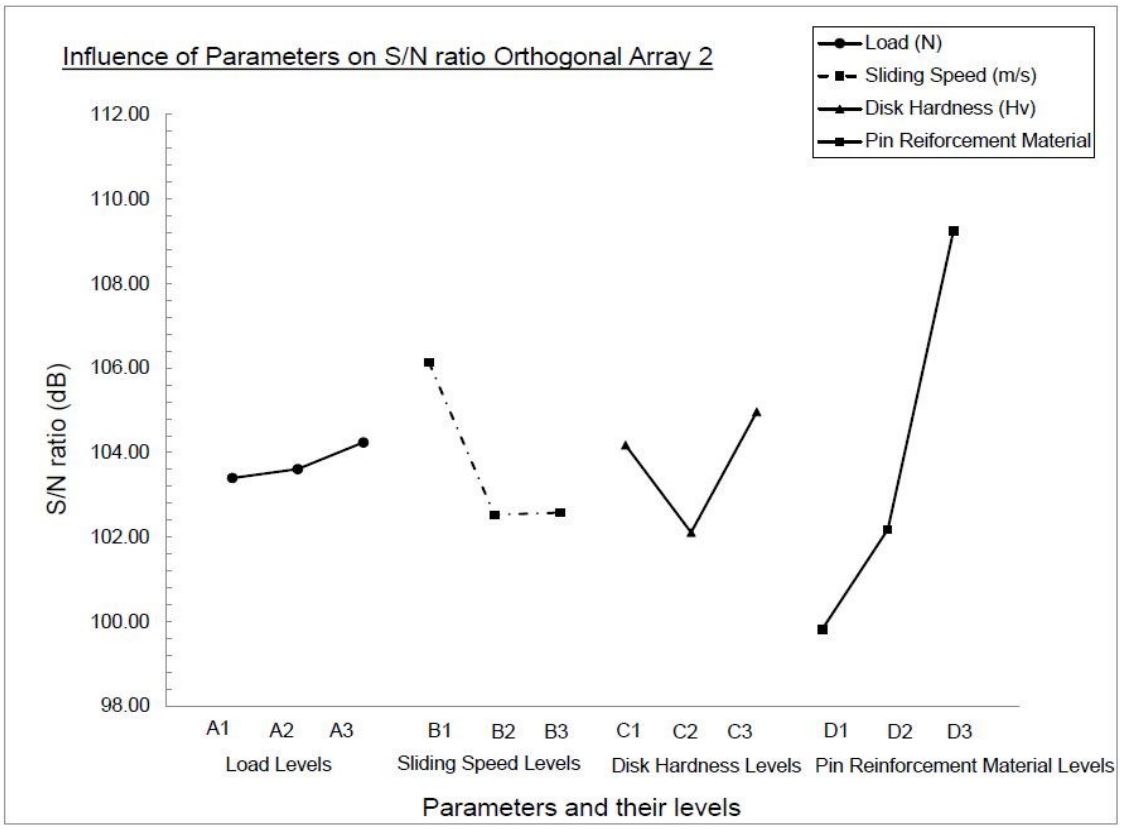

Figure 9 Mean S/N ratio for all parameters and their levels for low mass loss considering type of reinforced material

Again, an estimated S/N ratio was calculated, the results from the confirmation experiments for Orthogonal Array 2 can be found in Table 12.

Table 12. Results of confirmation tests for mass loss

	Optimal Parameters	
	Prediction	**Experiment**
S/N Ratio (dB)	107.84	106.44
Mass Loss (g)	0.0017	0.0020

As can be seen from Table 12 the predicted results were very accurate with the actual experimental results differing by only 17%, from the theoretical mass loss of 0.0017g to average recorded mass loss 0.0020g .

3.5 Residual Stresses

Residual stress measurements were carried out to allow an investigation into how load contributed towards residual stresses after wear test. Table 13 provides a summary of the results for the three additional wear tests.

Table 13 Residual stress measurements for additional wear testing trials with varying load

Load (N)	Average Normal Residual Stress Measured		Change in Normal Residual Stress (MPa)
	Parent Material (MPa)	Wear Scar (MPa)	
10	81.3	67.0	-14.30
20	94.2	74.5	-19.7
30	87.6	56.2	-31.4

3.5.1 Influence of Load on Residual Stresses

Figure 10 shows the normal residual stresses obtained post wear test.

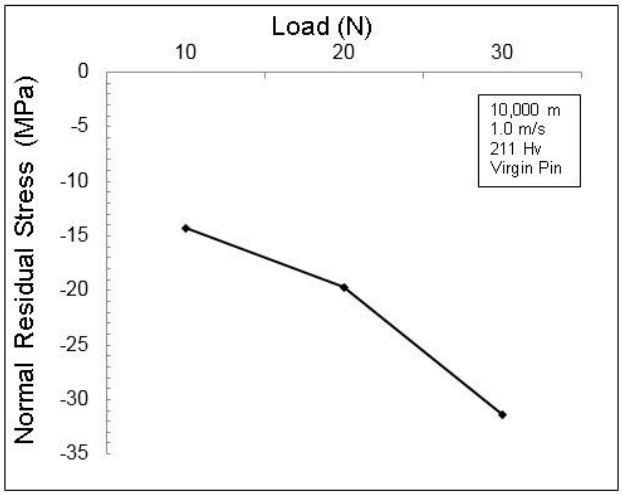

Figure 10 Variation in normal residual stresses vs load after conducting a wear test.

From Figure 10 it can be seen that as the load was increased during dry sliding the steel disk encountered larger compressive residual stresses. From the three load cases it can be said that the relationship between load and residual stresses incurred was fairly linear. This behaviour agree with research conducted by [12], who stated that the nature of the stresses in post wear testing metal matrix composites against a hardened steel disk was always compressive. The magnitude of residual stresses encountered in previous research [13] produced a large range of values with the lowest measuring -20MPa and the highest, -180MPa for varying load from 30N to 70N. Here the range is much smaller (-14MPa to -30MPa) due to the smaller values of loads used in this experiment.

4. Conclusions

In this research the wear resistance of two polymer composites, CF-PEEK and GF-PEEK were compared with the matrix polymer.

- Optimal values to produce the lowest amount of mass loss and as a consequence smallest wear rate, when considering wt.% carbon reinforcement are: low load of 10N, a low speed of 1.0m/s, a high steel disk hardness of 699HV and 20 wt.% carbon. Although a 20 wt.% carbon reinforcement was optimal, 30 wt.% carbon reinforcement followed closely on the S/N plot suggesting that there is minimal tribological benefit from the additional 10 wt.% carbon reinforcement.

- Optimal parameters required to produce the smallest mass loss and as a consequence smallest wear rate, when considering type of material reinforcement are: high load of 30N, a low speed of 1.0m/s, a medium steel disk hardness of 630HV and a glass reinforced PEEK pin.

- It was shown that the primary contributor on specific wear rate was wt.% reinforcement with ~74% of contribution, and similarly type of reinforcement material contributed for ~78%. Secondary contributor was the sliding speed with ~14%. Tertiary contributors were the load and disk hardness with a total contribution of less than 12%.

- An investigation into the presence and nature of residual stresses post wear testing found that the residual stresses were compressive in nature, with their magnitude increasing as load was increased. Despite the low load values there was still a change in residual stresses detected.

Acknowledgments: The authors would like to acknowledge the contribution of the University of Strathclyde for providing both equipment and support throughout the project. Also a special thanks to Victrex for providing all polymer samples known as VICTREX® PEEK.

Funding: “This research received no external funding”

5. References

[1] Gupta, R.K. Kennel, E; Kim, K.J. (2009). Polymer nanocomposites handbook. CRC Press, Boca Raton, Florida

[2] Unal, H., U. Sen, & A. Mimaroglu. (2004). Dry sliding wear characteristics of some industrial polymers against steel counterface. Tribology International. 37(9): Pp. 727-732

[3] Lu, Z.P. and Friedrich, K. (1995). On sliding friction and wear of PEEK and its composites. Wear. 181–183, Part 2(0): Pp. 624-631.

[4] Davim, J.P. and Cardoso, R. (2006). Tribological behaviour of the composite PEEK-CF30 at dry sliding against steel using statistical techniques. Materials & Design. 2006 27(4): p. 338-342.

[5] Davim, J.P. and Cardoso, R. Effect of the reinforcement (carbon or glass fibres) on friction and wear behaviour of the PEEK against steel surface at long dry sliding. Wear. 2009, 266(7–8): Pp. 795-799

[6] Wang, Z. and D. Gao. (2014). Friction and wear properties of stainless steel sliding against polyetheretherketone and carbon-fiber-reinforced polyetheretherketone under natural seawater lubrication. Materials & Design, 2014. 53: p. 881-887

[7] Li, E.Z., et al. (2013). Research on Tribological Behaviour of PEEK and Glass Fiber Reinforced PEEK Composite. Physics Procedia. 50: p. 453-460.

[8] Shaw B.A; Aylott, C; O'Hara, P and Brimble, K. (2003). The role of residual stress on the fatigue strength of high performance gearing, International Journal of Fatigue, Volume 25, Issues 9–11, Pp 1279-1283

[9] James, M.N. Hughes, D.J. Chen, Z. Lombard, H. Hattingh, D.G. Asquith, D. . Yates, J.R Webster, P.J. (2007). Residual stresses and fatigue performance, Engineering Failure Analysis, Volume 14, Issue 2, Pp 384-395

[10] Shokrieh, M.M. and Ghanei Mohammadi, A.R. (2014). The importance of measuring residual stresses in composite materials, in Residual Stresses in Composite Materials, M.M. Shokrieh, Editor. Woodhead Publishing. Pp. 3-14.

[11] LeMaster R., Boggs B., Bunn J., Hubbard C., Watkins T. (2009). Grinding Induced Changes in Residual Stresses of Carburized Gears, Gear Technology, 26 – 2, Pp. 42-49.

[12] Ho J.W., Noyan, C; Cohen J.B; Khanna, V.D; Eliezer, Z. (1983). Residual Stresses and Sliding Wear. Wear, Vol. 84, Issue 2, Pp 183-202

[13] Vanarotti, P. Shrishail, B.R. Sridhar, and Kori, S.A. (2014). Study of Mechanical Properties & Residual Stresses on Post Wear Samples of A356-SiC Metal Matrix Composites, Procedia Materials Science, Volume 5. Pp 873-882

[14] Kassfeldt E, Paper XVIII (i). (1987). The influence of back-up rings on the hydrodynamic behaviour of hydraulic cylinder seals, In: D. Dowson, C.M. Taylor, M. Godet and D. Berthe, Editor(s), Tribology Series, Elsevier, Volume 11, Pp 545-551

[15] ISO 14707:2015. Surface Chemical Analysis-Glow Discharge optical Emission Spectrometry (GD-OES)

[16] Saxon Steels LTD, A.I.S.I. 0-1 Ground Flat Tool Steel. Datasheet, July 2006

[17] ASTM (2001). Standard Guide for Preparation of Metallographic Specimens. ASTME3-01.

[18] ASTM (2003). Standard Test Method for Vickers Hardness of Metallic Materials. ASTM E92-82. 2003.
[19] ASTM (2004). Standard Test Method for Wear Testing with a Pin on Disk Apparatus ASTM G99-04.
[20] Minitab 18. Support. Available at https://support.minitab.com/en-us/minitab/18/help-and-how-to/modeling-statistics/doe/supporting-topics/taguchi-designs/what-is-the-signal-to-noise-ratio/ [accessed: 15 October 2018]
[21] Fitzpatrick, M.E. Fry A.T. and Holdway,P. (2005). Measurement Good Practice Guide No. 52. Determination of residual stresses by X-ray diffraction – Issue 2 (Report) National Physical Laboratory, Teddington (UK)
[22] Prevéy, P.S. (1986). X-ray diffraction residual stress techniques. ASM International Handbook, 10, Pp 380-392.
[23] Prevéy, P.S. (1986). The use of Pearson VII distribution functions in X-ray diffraction residual stress measurement. Advances in X-ray Analysis, 29, Pp.103-111
[24] Tang, L; Gao, C; Huang, J; Zhang, H; Chang, W. (2013). Dry sliding friction and wear behaviour of hardened AISI D2 tool steel with different hardness levels, Tribology International, Volume 66, Pp. 165-173
[25] Suh N.P. (1986). Tribophysics, Prentice-Hall, Englewood Cliffs, NJ,